

Towards establishing a long-term cloud record from space-borne lidar observations

Artem Feofilov¹, Helene Chepfer¹,
Vincent Noel², and Frederic Szczap³

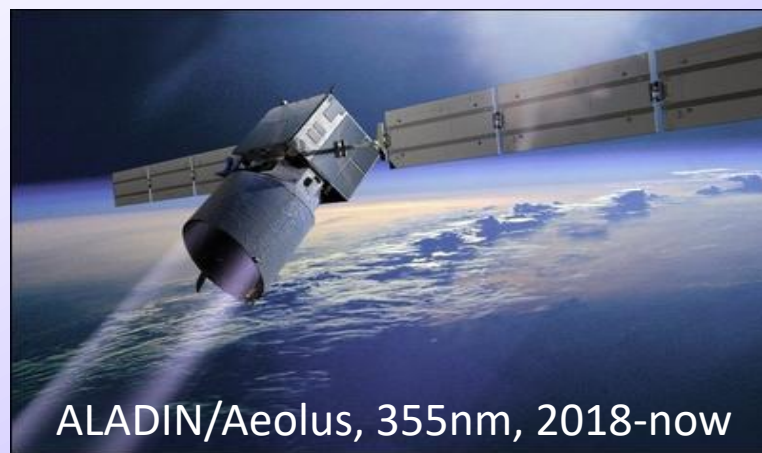
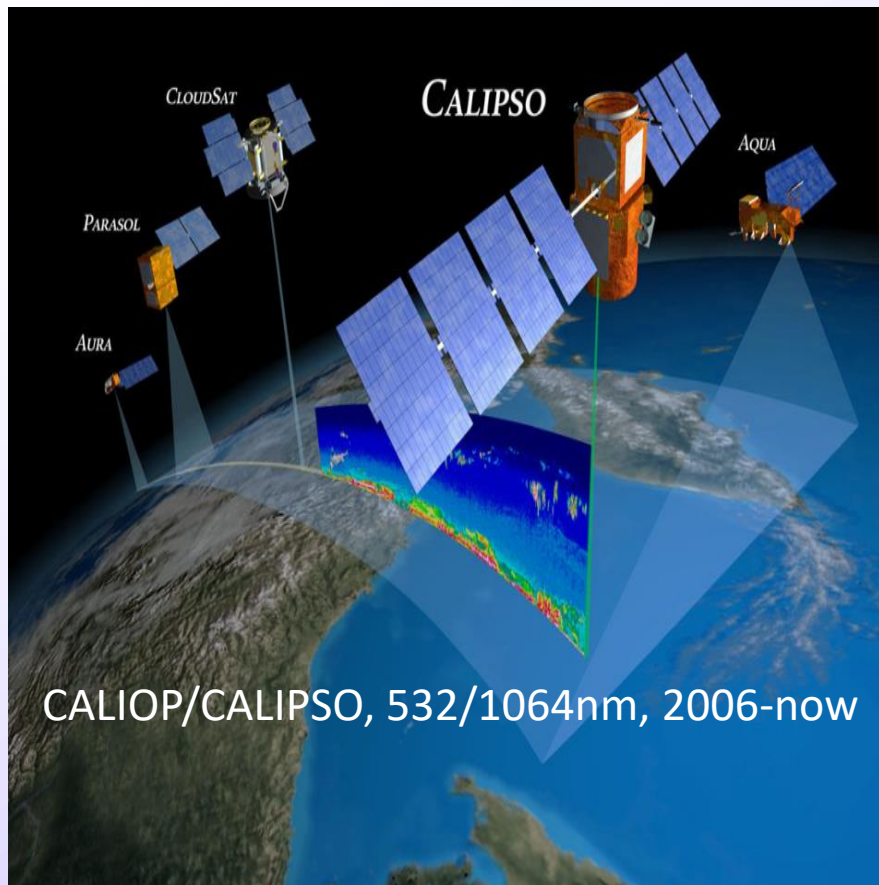
with contribution of Maryam Hajiaghazadeh-Roodsari¹

1 – LMD / Sorbonne Université / IPSL / Ecole Polytechnique

2 – Laboratoire d'Aérodynamique, CNRS/UPS, Observatoire Midi-Pyrénées, Toulouse

3 – Laboratoire de Météorologie Physique, CNRS, Aubière

Continuous cloud record from space-borne lidars



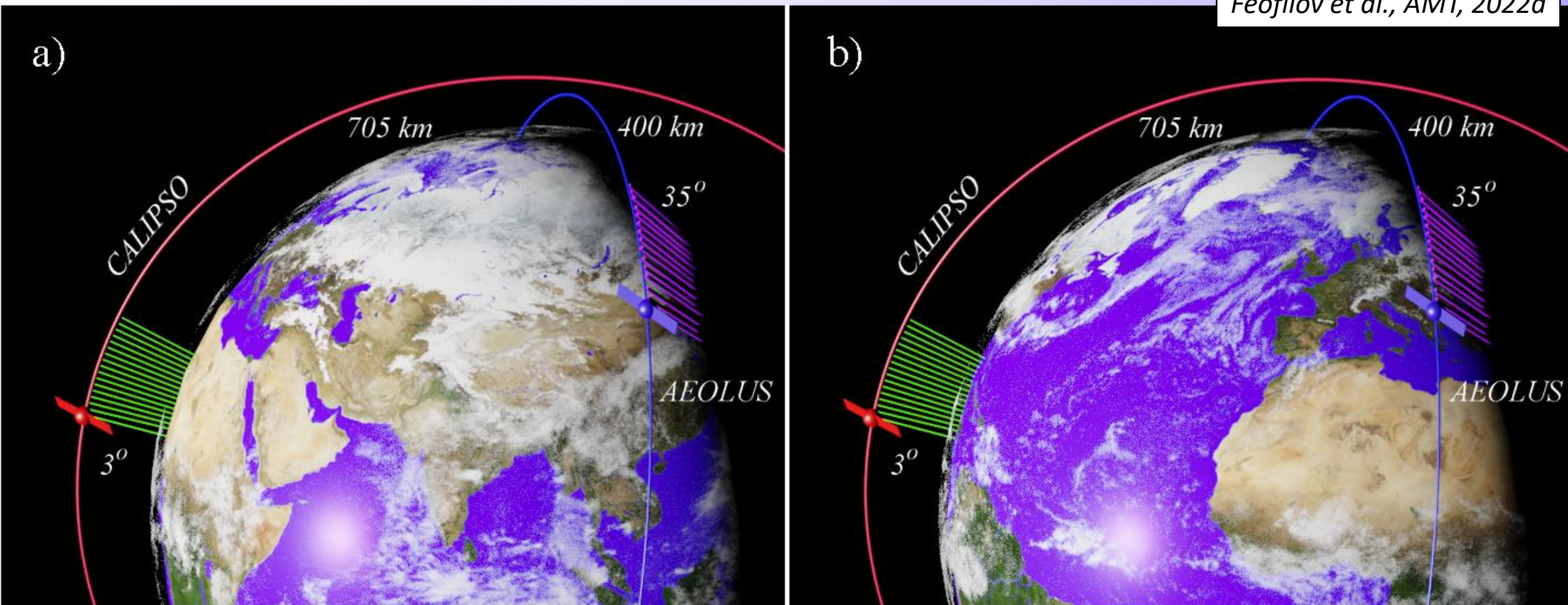
- General principle is the same: polar orbit, 15 tracks per day, sounding radiation is sent downwards, the backscattered signal is sampled and interpreted.

- Differences between lidars: **wavelength**, **observation geometry and time**, **HSRL capability**, **averaging distance**, **vertical resolution**, **noise**.



Differences between CALIPSO and AEOLUS

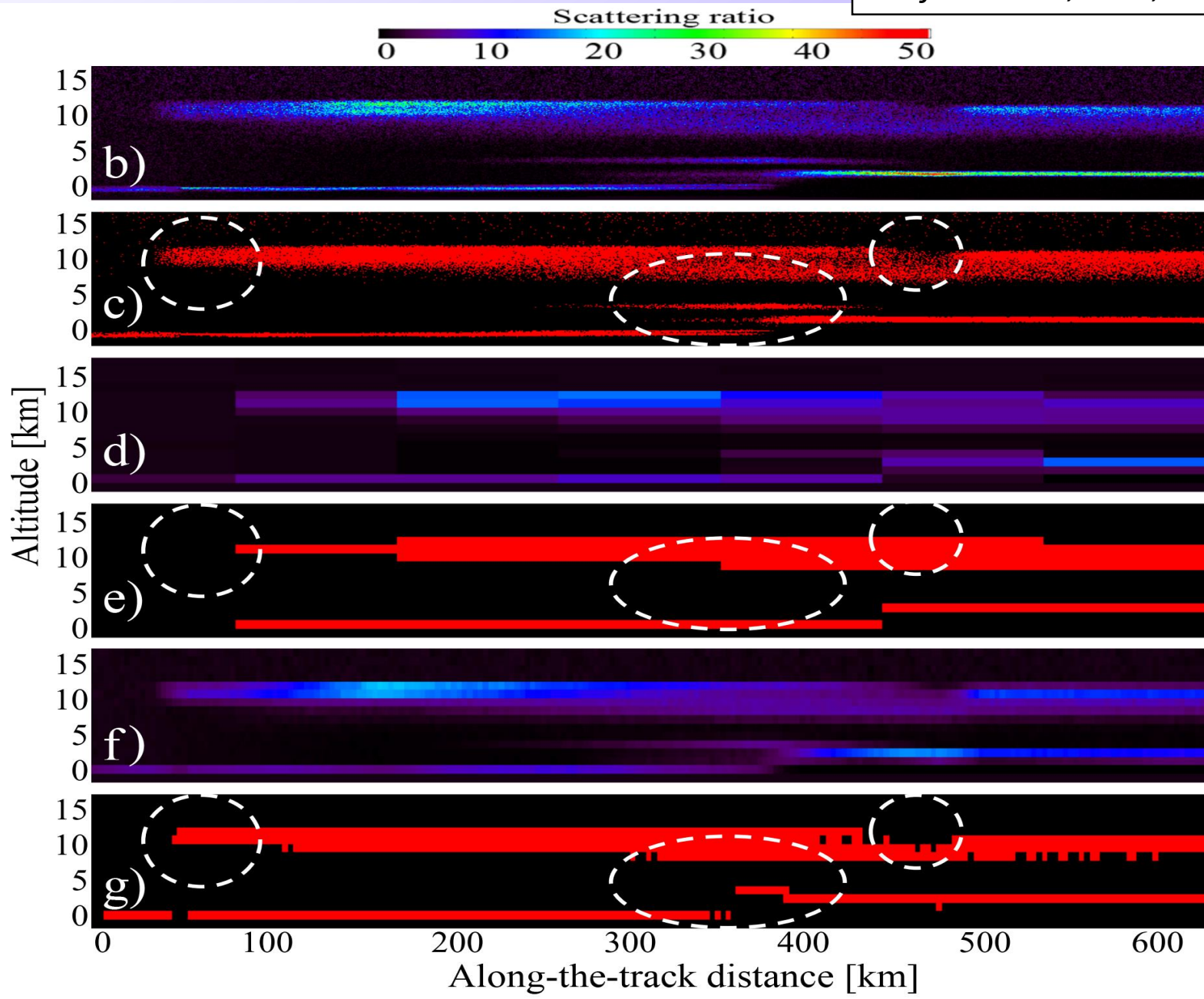
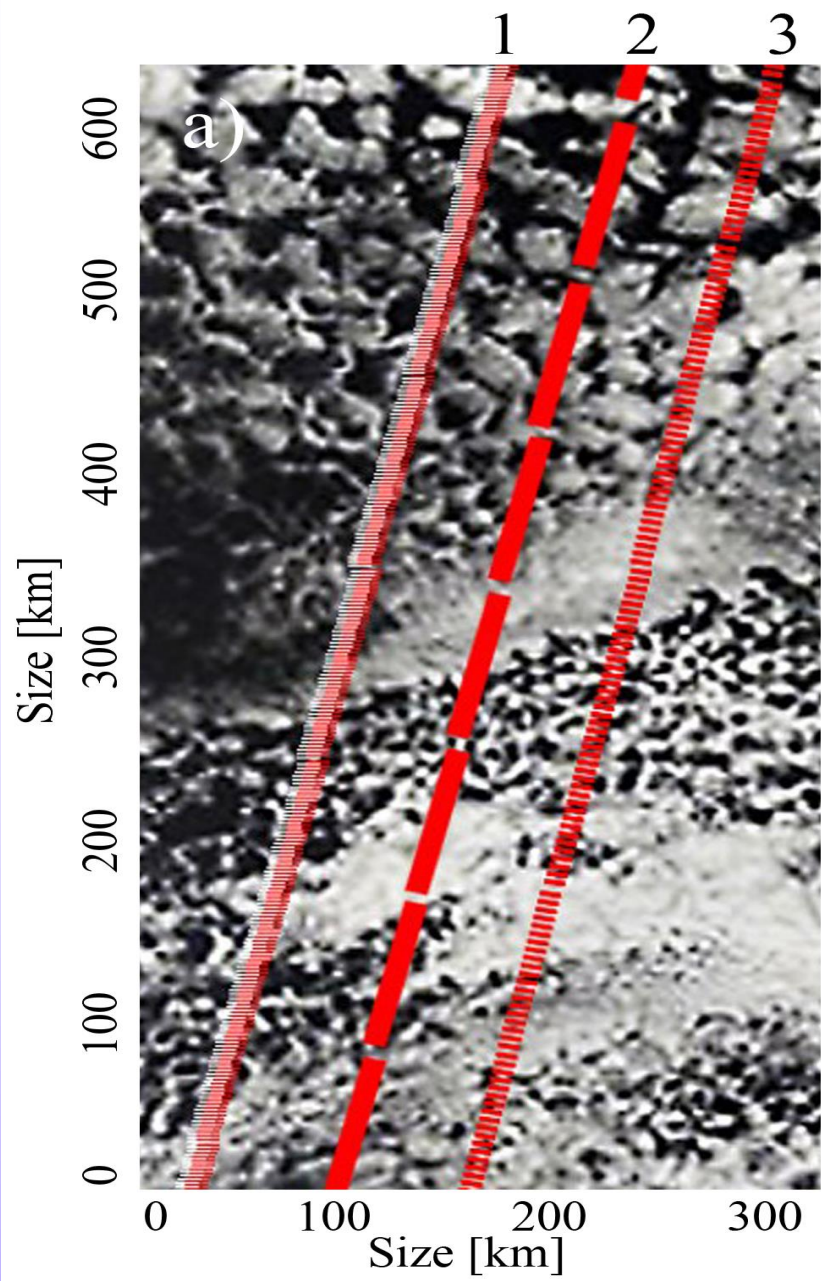
Feofilov et al., AMT, 2022a



Observation geometry and orbits of ALADIN/Aeolus and CALIOP/CALIPSO space borne lidars. ALADIN observes the atmosphere at dawn-dusk, whereas CALIOP passes the equator at 01:30 and 13:30 local solar time. The difference between (a) and (b) panels is in the position of Earth and the time: in (b), AEOLUS overflies the same area (centered over Africa) as was observed by CALIOP ~4.5 h earlier (in (a)).

Differences associated with averaging

Feofilov et al., AMT, 2022a



Estimating scattering ratio at 532nm

ALADIN L2A algorithm retrieves particle backscatter and extinction at 355nm, whereas we want to compare the clouds estimated from scattering ratio at 532nm

$$SR^C(\lambda, z) = \frac{ATB(\lambda, z)}{AMB(\lambda, z)}$$

Scattering ratio definition

$$ATB(\lambda, z) = (\beta_{mol}(\lambda, z) + \beta_{part}(\lambda, z)) \times e^{-2 \int_{z_{sat}}^z (\alpha_{mol}(\lambda, z') + \eta \alpha_{part}(\lambda, z')) dz'}$$

Lidar equation

$$AMB(\lambda, z) = \beta_{mol}(\lambda, z) \times e^{-2 \int_{z_{sat}}^z \alpha_{mol}(\lambda, z') dz'}$$

Attenuated molecular backscatter in absence of particles

$$\beta_{mol}(\lambda, z) = (d\sigma/d\Omega)_\lambda \times N(z); \quad \alpha_{mol}(\lambda, z) = \frac{4\pi}{1.5} \beta_{mol}(\lambda, z)$$

$$(d\sigma/d\Omega)_\lambda = \frac{\sigma(\lambda, z)}{4\pi} \times \frac{3}{4} (1 + \cos^2(\pi))$$

$$\sigma(\lambda, z) = \frac{24\pi^3 (n_s^2(\lambda) - 1)^2 (6 + 3\rho(\lambda))}{\lambda^4 N_s^2 (n_s^2(\lambda) + 2)^2 (6 - 7\rho(\lambda))}$$

Calculating molecular backscatter and extinction coefficients

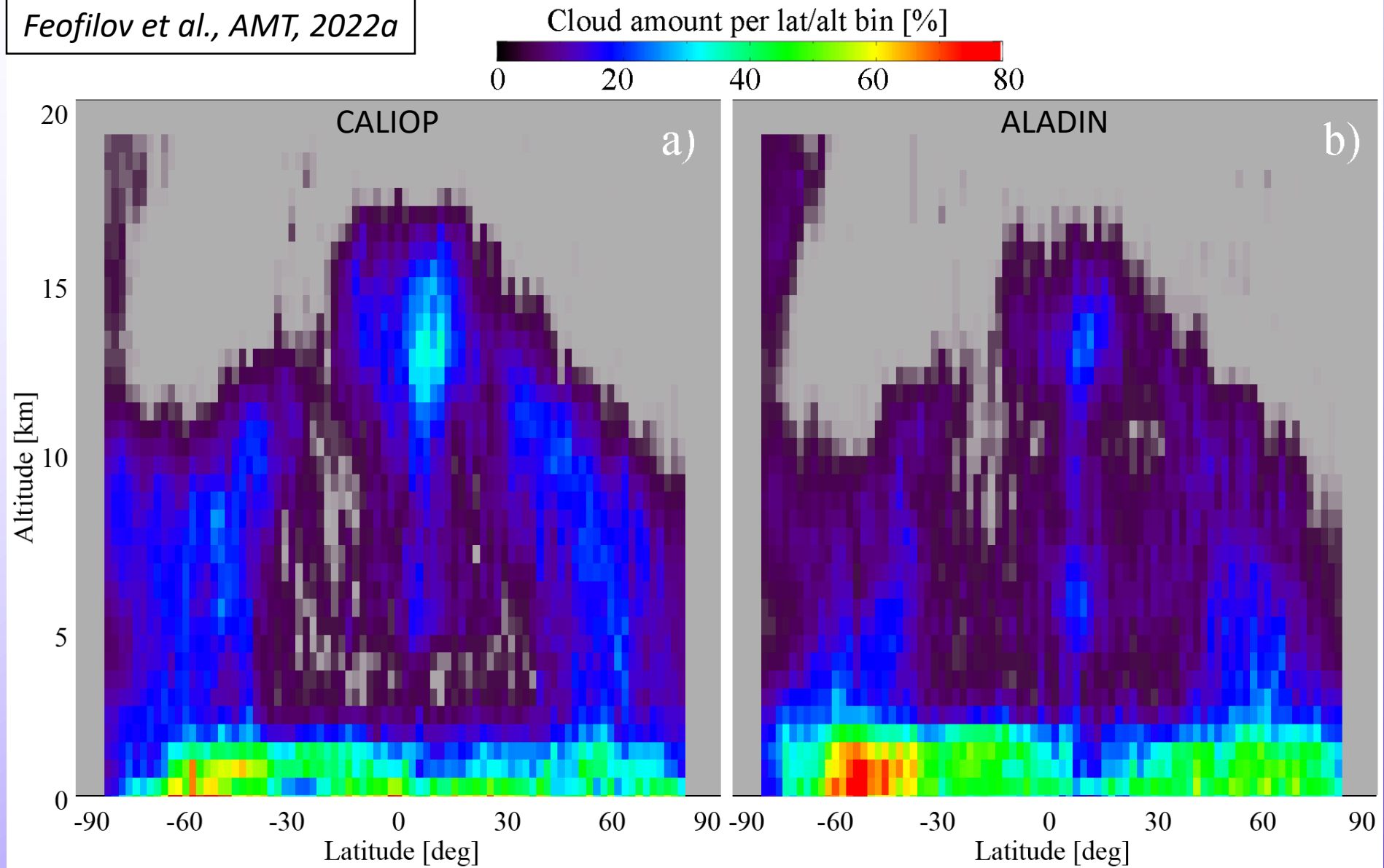
$$\alpha_{part}(355\text{nm}, z) \approx \alpha_{part}(532\text{nm}, z) \quad \beta_{part}(355\text{nm}, z) \approx \beta_{part}(532\text{nm}, z)$$

$$SR(532\text{nm}, z) > 5$$

Threshold is applied to “native” and converted SR values

Cloud amount estimated from CALIOP and ALADIN

Feofilov et al., AMT, 2022a



The same cloud detection threshold $SR > 5$ applied to SR profiles at the same vertical and horizontal resolutions (Chepfer et al. 2013)

Accounting for depolarisation effects

ADM-AEOLUS Science Report, 2008

Flamant et al., 2021

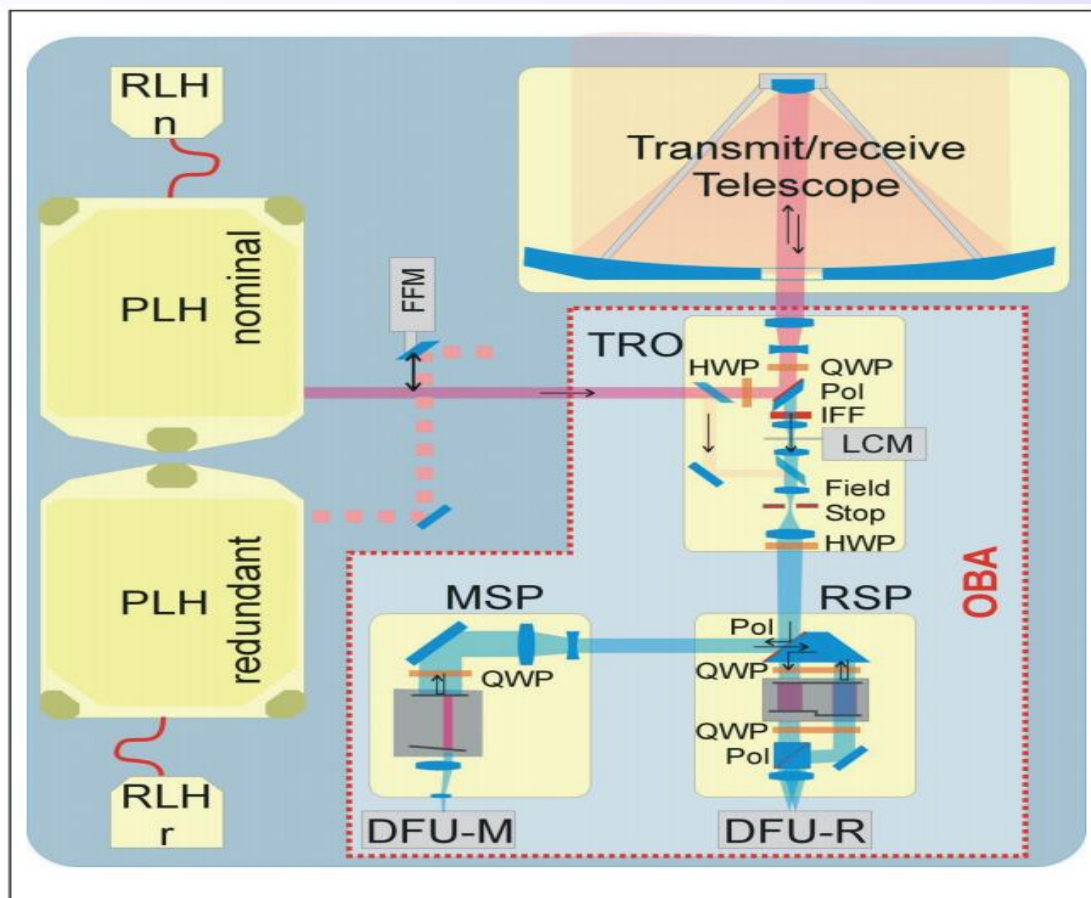


Fig. 4.13. Optical architecture of ALADIN. PLH: Power Laser Head, RLH: Reference Laser Head, FFM: Flip-Flop Mirror, LCM: Laser Chopper Mechanism, TRO: Transmit/Receive Optics, RSP: Rayleigh Spectrometer, DFU: Detection Front-end Unit, QWP: Quarter-Wave Plate, HWP: Half-Wave Plate, Pol: Polariser, IFF: Interference Filter.

3 Known limitations

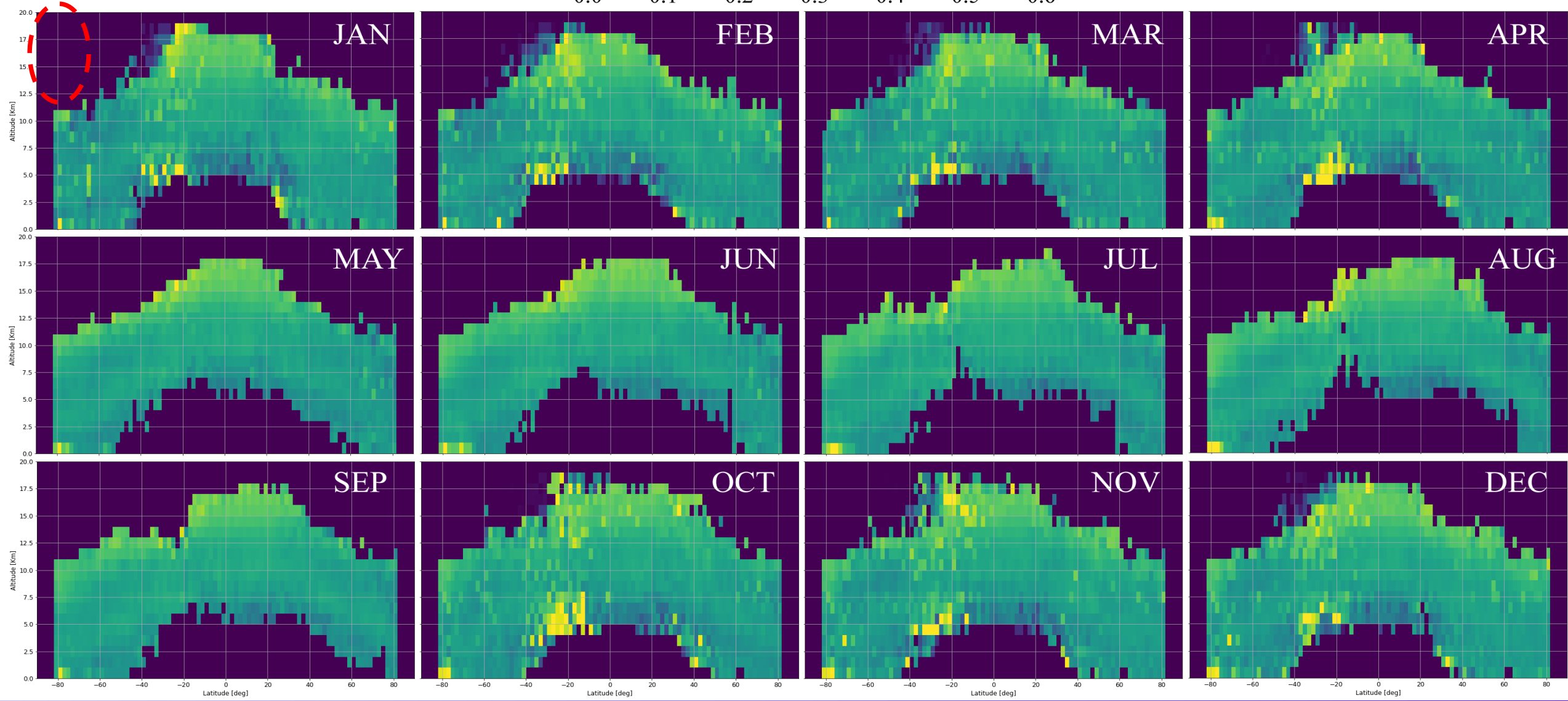
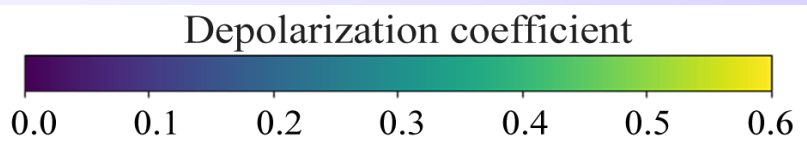
3.1 Instrument limitations

ALADIN was designed primarily for wind determination. The fraction of light sent through the Fizeau interferometer of the Mie channel is smaller than for the Rayleigh channel. The Mie SNR is then lower than the Rayleigh SNR and limits the precision of signals calculated through the cross-talk correction.

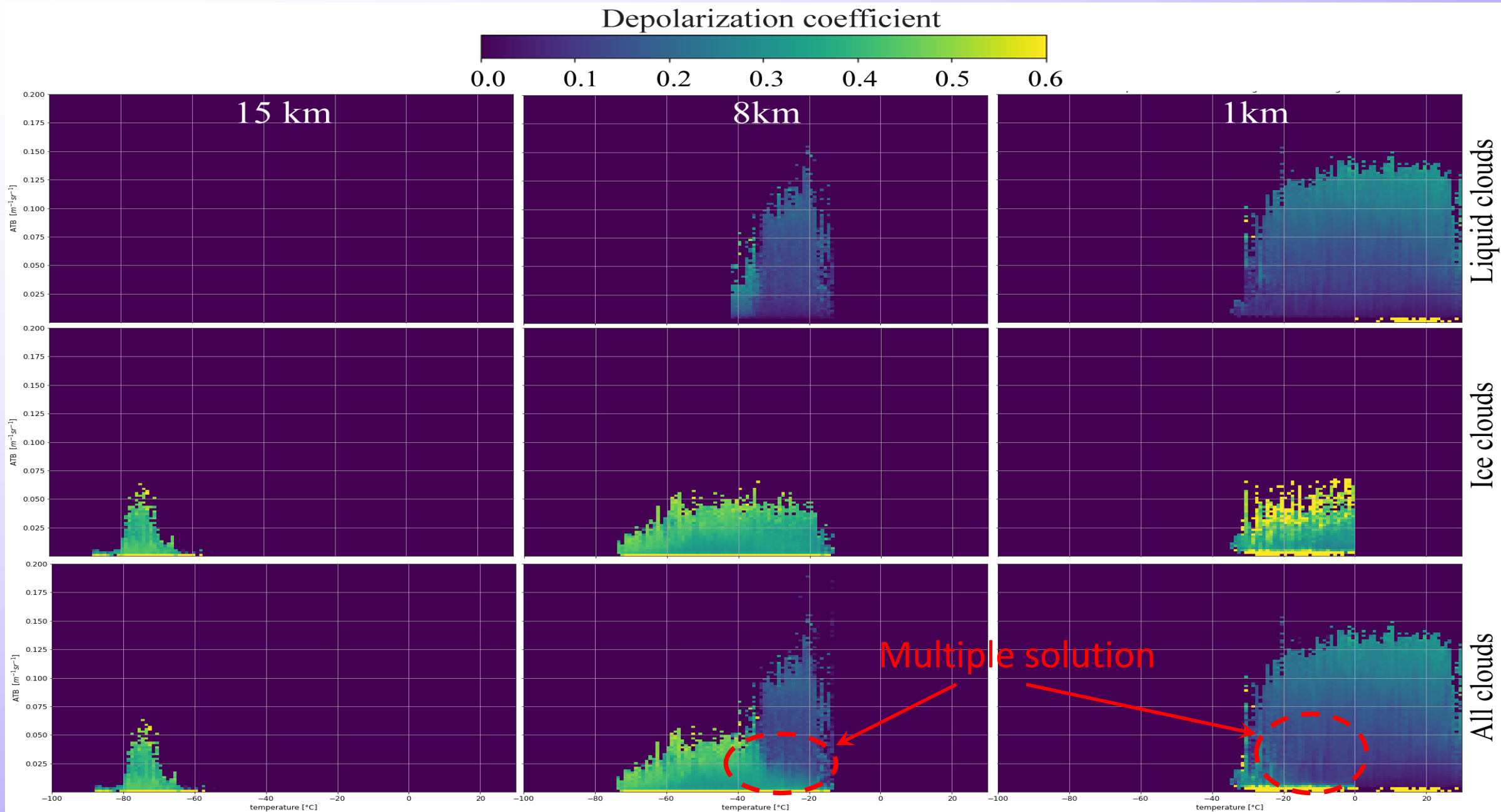
Designed as a wind lidar, ALADIN was not initially aimed at observing aerosol optical properties in detail. Under these requirements, it was not fitted with the ability to measure depolarization. The UV laser beam is linearly polarized at the laser output. It goes through a quarter-wave plate (see Fig. 4.13 in ESA, 2008) before being routed towards the telescope and is thus transmitted towards the atmosphere with a circular polarization. On the way back, backscattered light goes again through the quarter-wave plate. The circularly polarized light that was transmitted might come back elliptically polarized in the case it was backscattered by depolarizing targets. After going through the quarter-wave plate, it becomes a mix of linearly polarized light, either along the same

Accounting for depolarisation effects – climatology $\delta(\text{month}, \text{lat}, Z)$

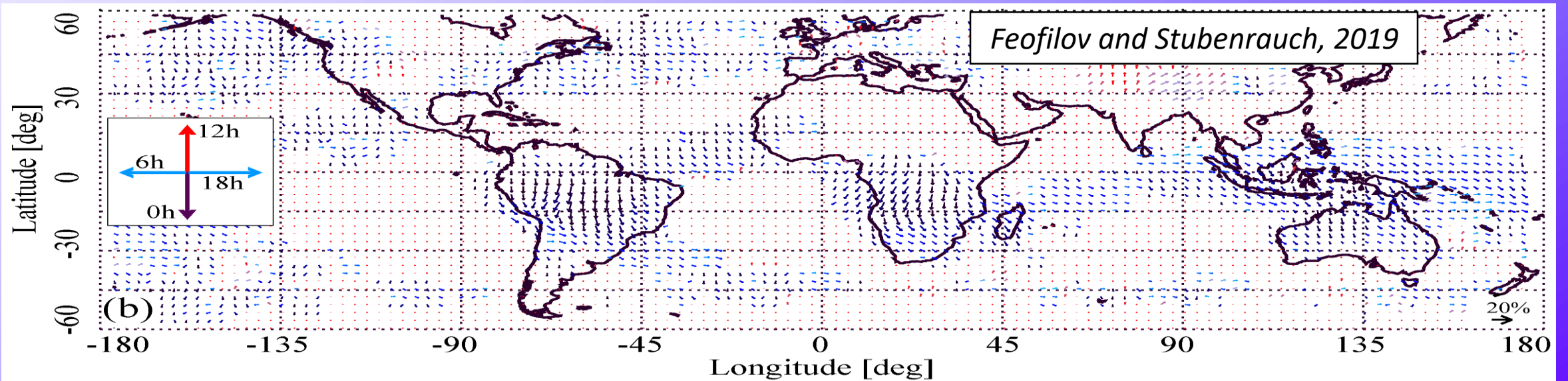
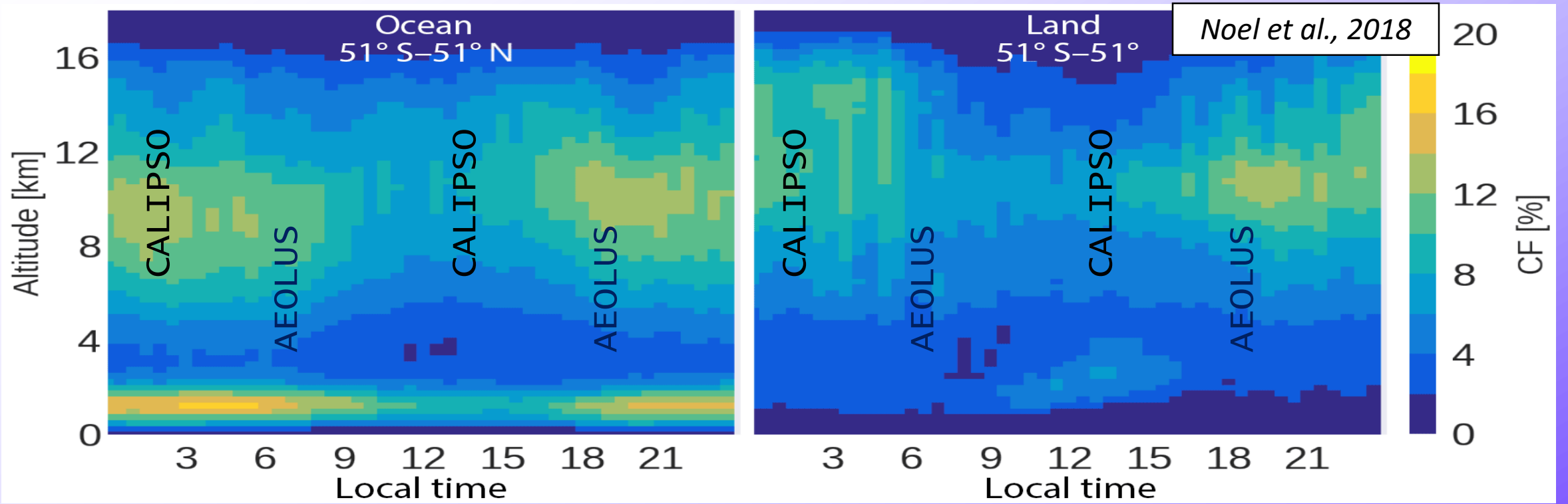
PSC area excluded on purpose



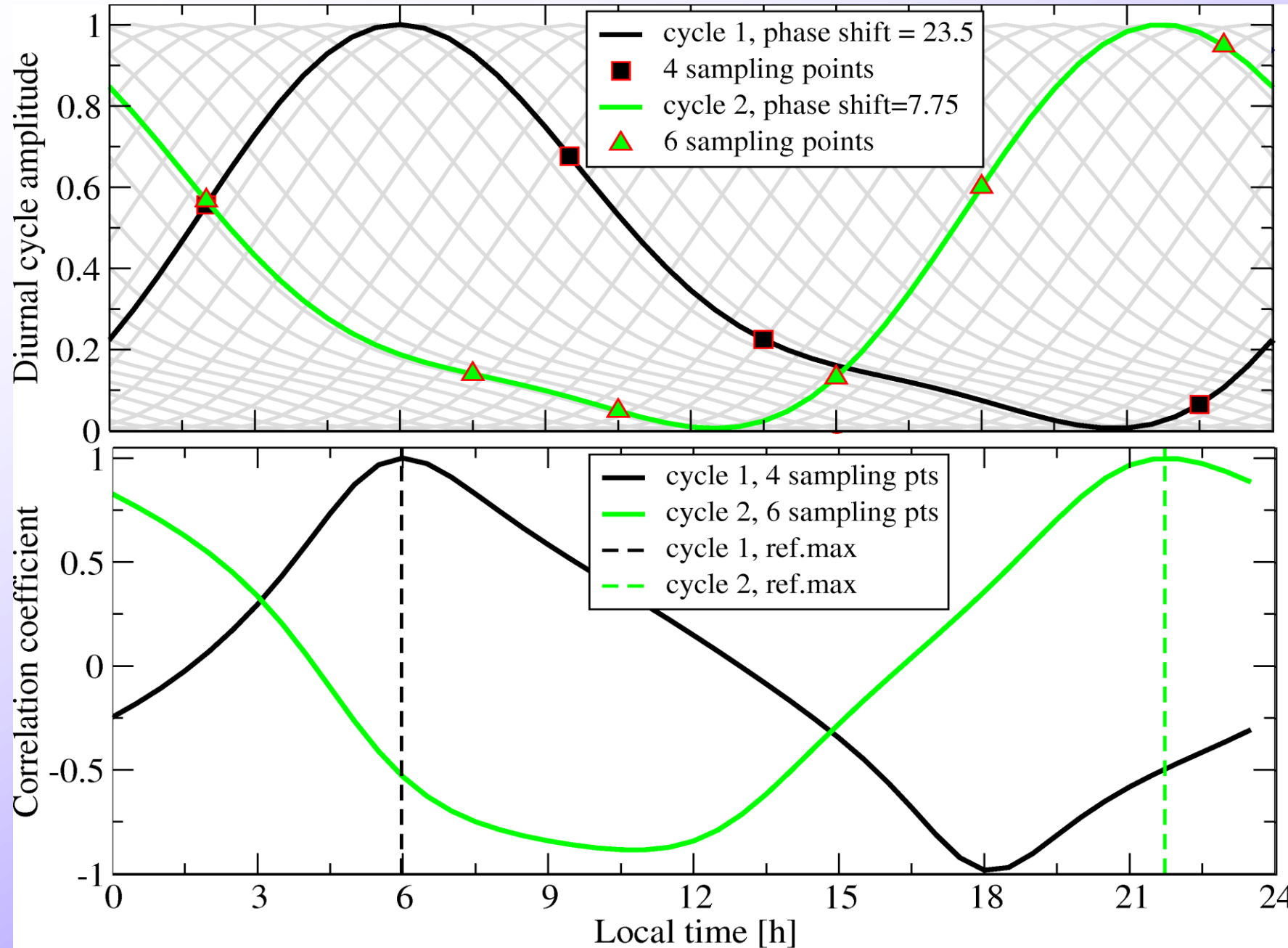
Accounting for depolarisation effects – parameterization $\delta(T, ATB, Z)$



Diurnal cycle of clouds and difference in overpass time



Diurnal cycle retrieval approach for any (lat,lon,height) bin



Feofilov and Stubenrauch, 2019

$$A(t) = A_{24} \cdot \sin\left(\frac{2\pi}{24}t + \varphi_{24}\right) + A_{12} \cdot \sin\left(\frac{2\pi}{12}t + \varphi_{24} + \Delta\varphi\right)$$
$$= A_{24} \cdot \left[\sin\left(\frac{2\pi}{24}t + \varphi_{24}\right) + 0.28 \cdot \sin\left(\frac{2\pi}{12}t + \varphi_{24} + \Delta\varphi\right) \right]$$

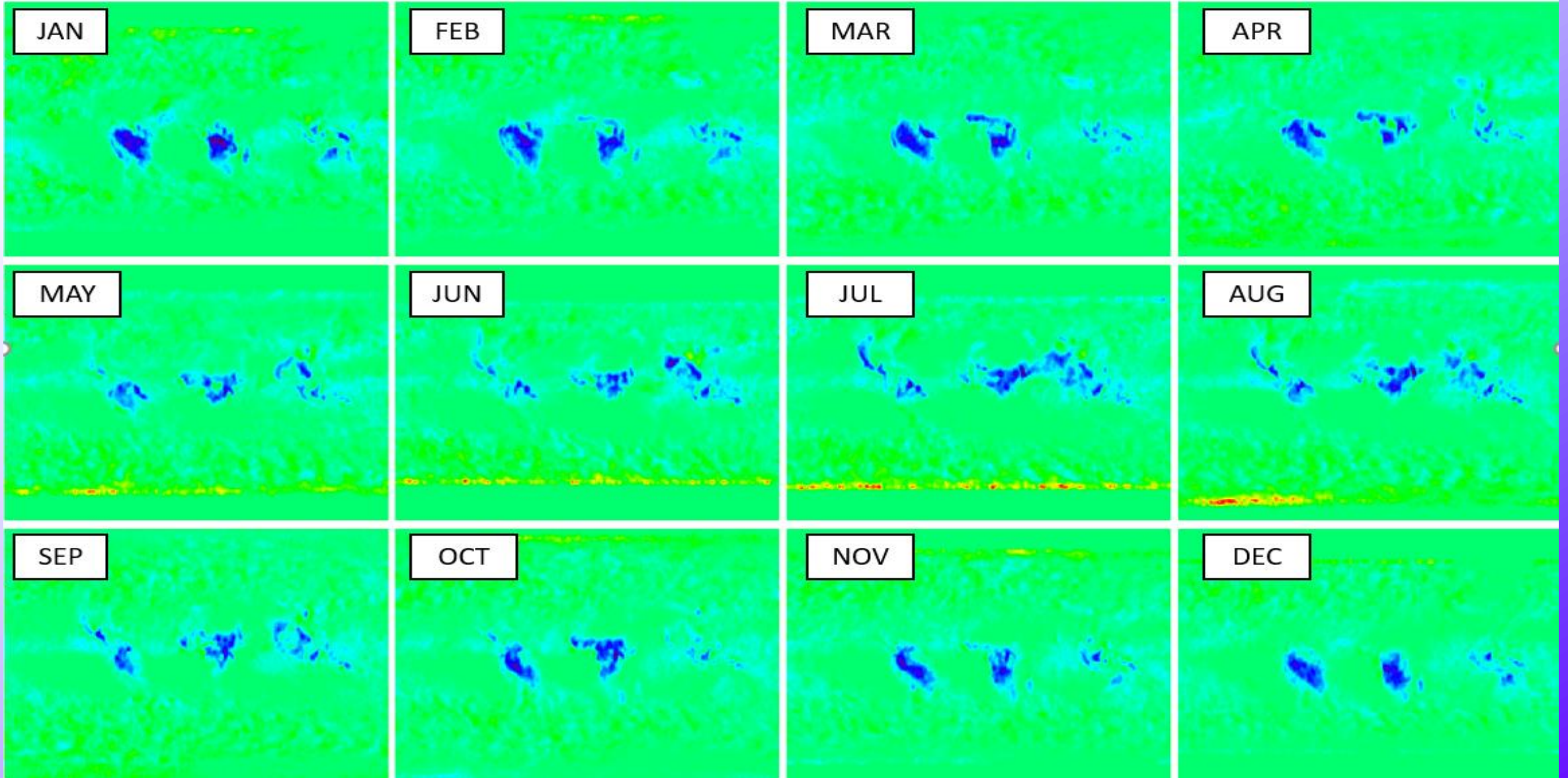
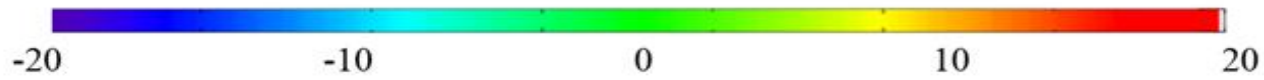
The "standard shape" comes from (Cairns, 1995)

The methodology has been applied to high clouds from AIRS/IASI data (Feofilov and Stubenrauch, 2019) and to **vertically resolved** CATS data (Noel et al., 2018)

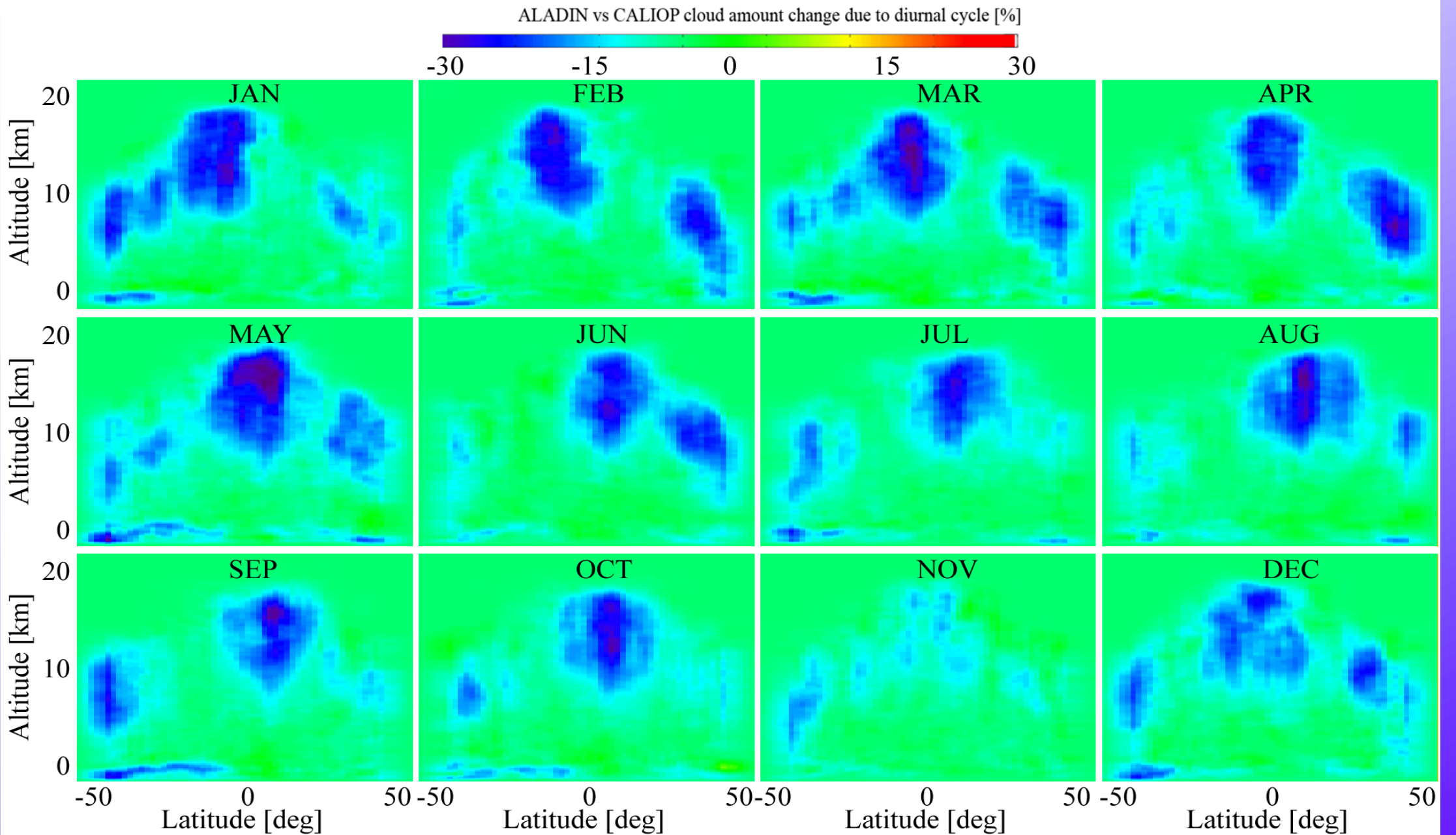
Two $1^\circ \times 1^\circ$ gridded datasets (A_{24} and φ_{24}) are available for download

Diurnal cycle correction for high clouds from AIRS/IASI

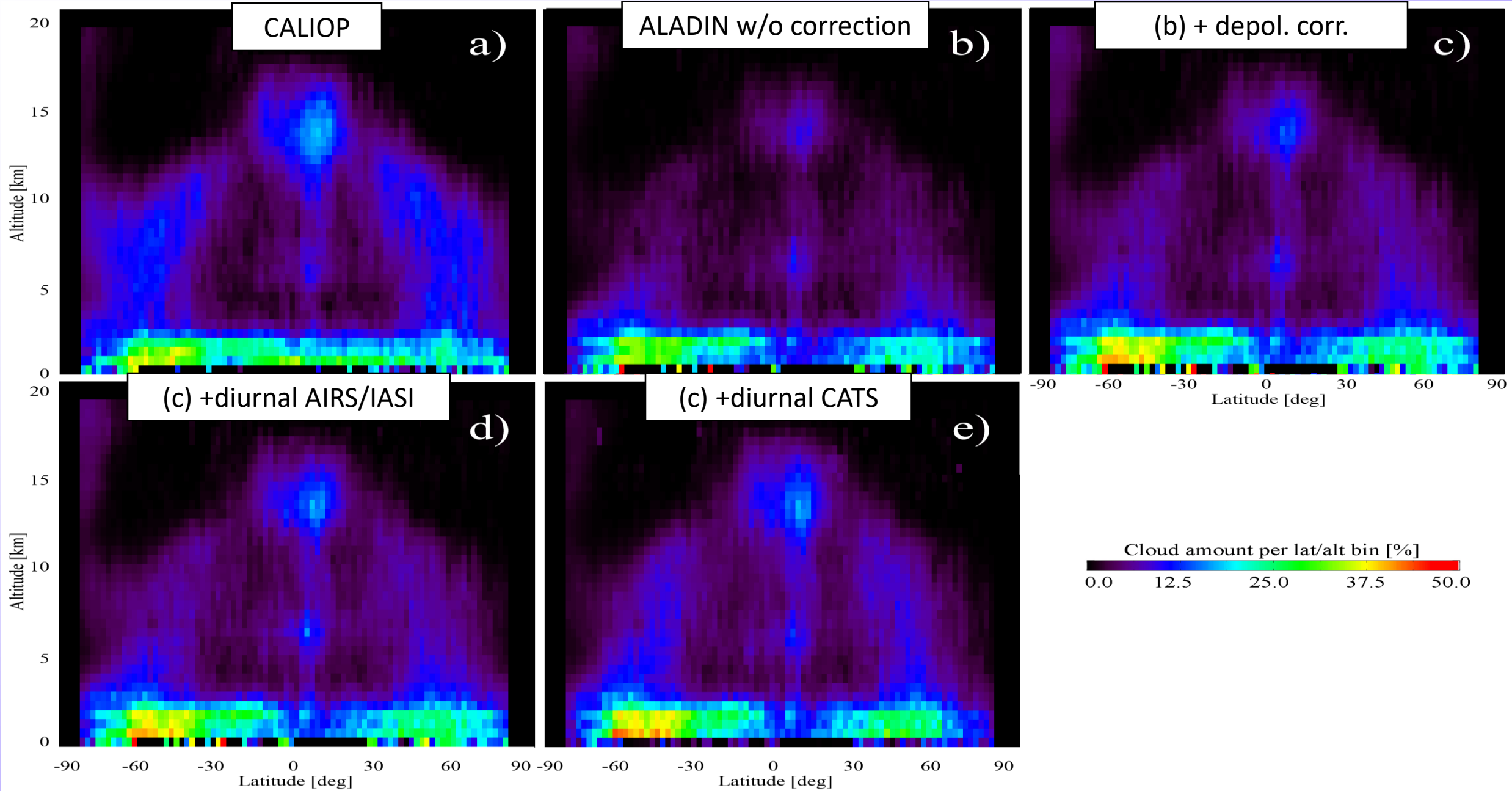
ALADIN vs CALIOP cloud amount change due to diurnal cycle [%]



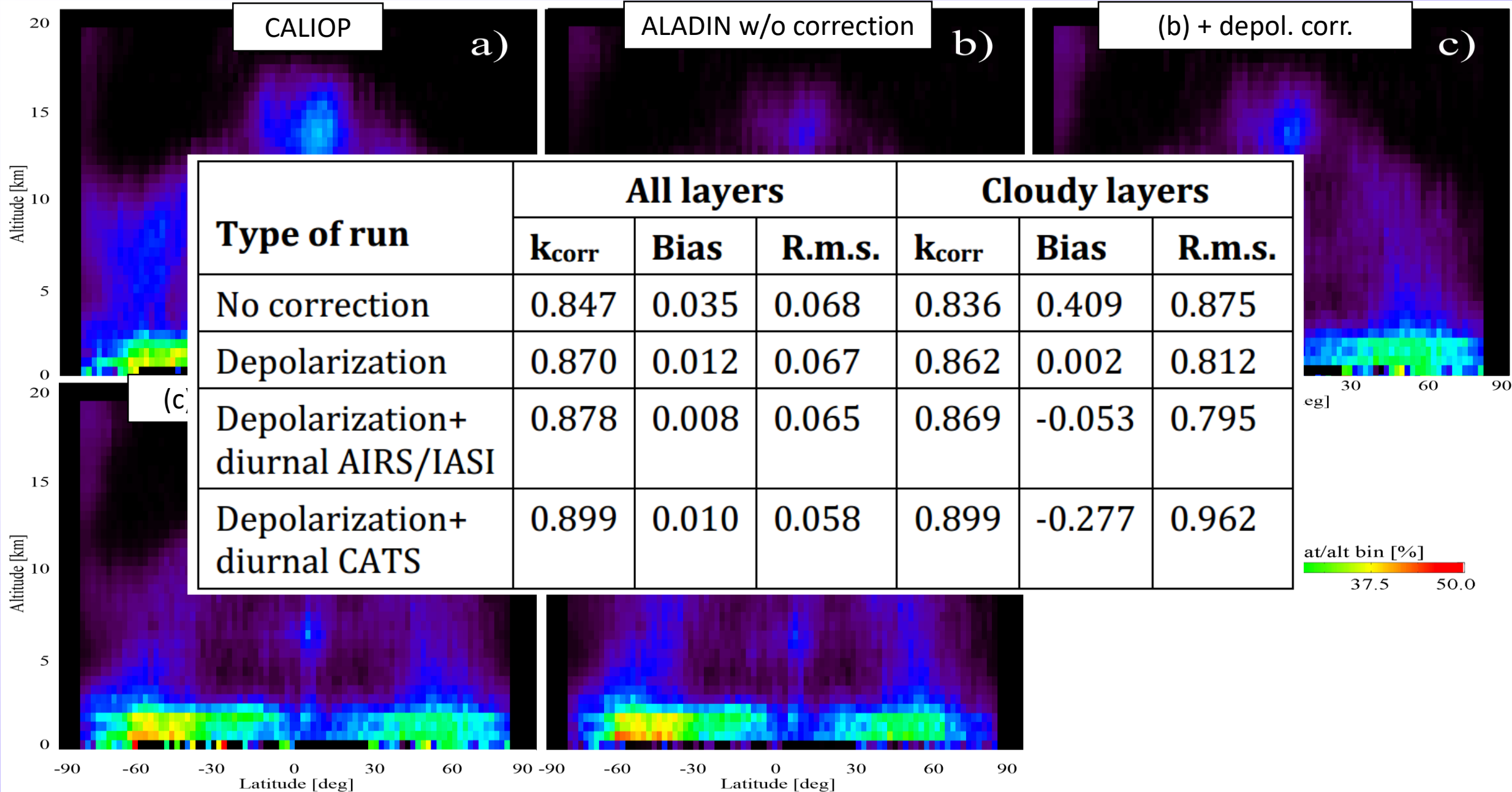
Height-resolved diurnal cycle correction from CATS



Depolarization- and diurnal cycle- corrected cloud amounts



Depolarization- and diurnal cycle- corrected cloud amounts



Merging cloud record with future lidars

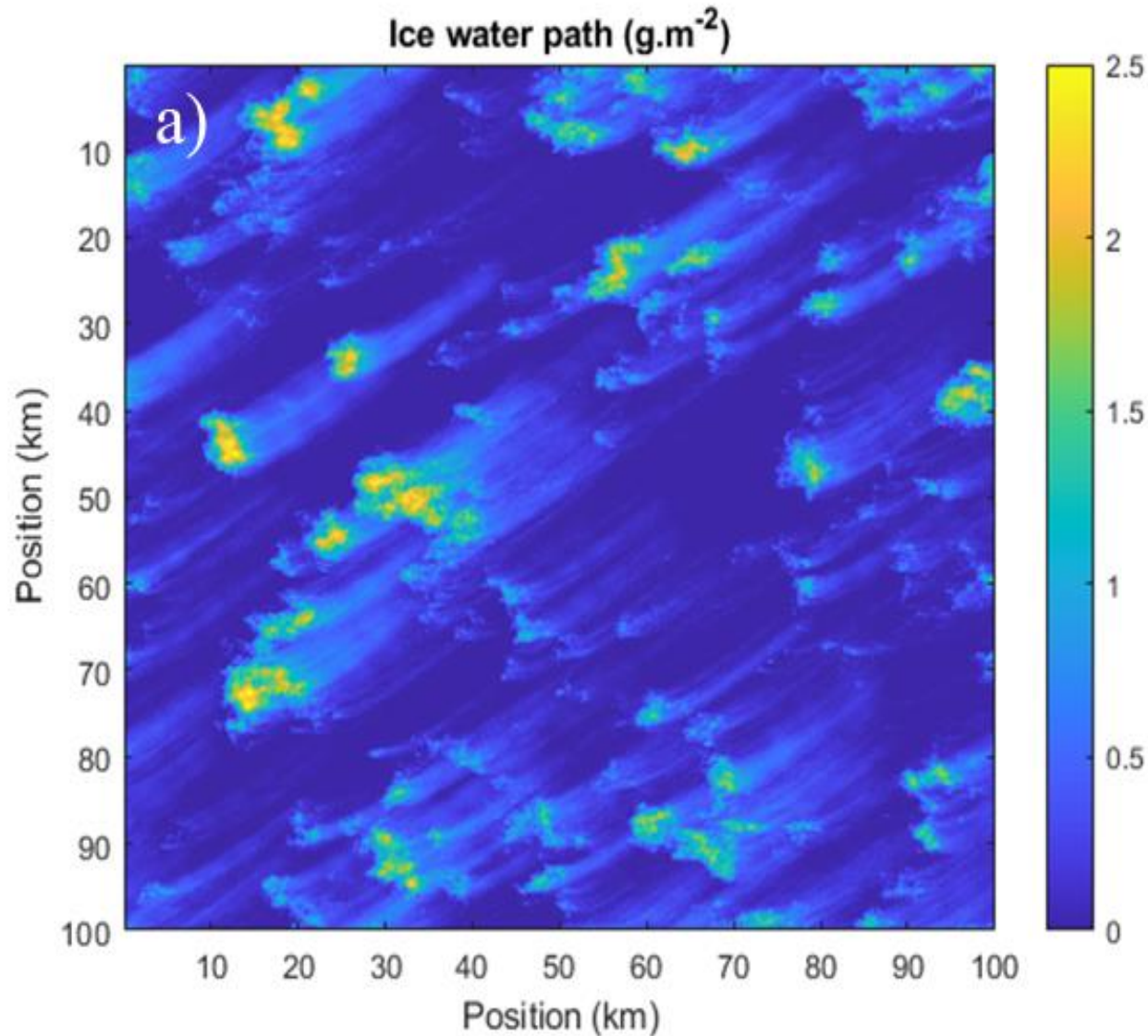
What to expect from ATLID w.r.t. CALIPSO ?

Parameter	CALIOP	ATLID
Altitude, [km]	690	393
Orbital inclination, [deg]	98.05	97.050
Wavelength, [nm]	532/1064	355
Pulse Repetition Frequency, [Hz]	20	51 (25.5)*
Horizontal distance between profiles, [m]	333	285
Finest Vertical resolution (troposphere), [m]	30	100
Telescope diameter, [m]	0.85	0.6
Telescope Field of view, [μ rad]	130	64
Energy/pulse, [mJ]	110	35 (70)*
Footprint, [m]	90	29
Laser beam divergence [μ rad]	100	45
Solar filter bandwidth, [nm]	0.04/0.475	0.71 (0.35)**
Total optical system loss coefficient	0.67/0.68	0.62
Detector efficiency	0.109/0.4	0.85
Dark current, [phot/s]	1331/1.85e7	153

Sources : Winker et al. (2009) for CALIOP and do Carmo et al. (2021) for ATLID

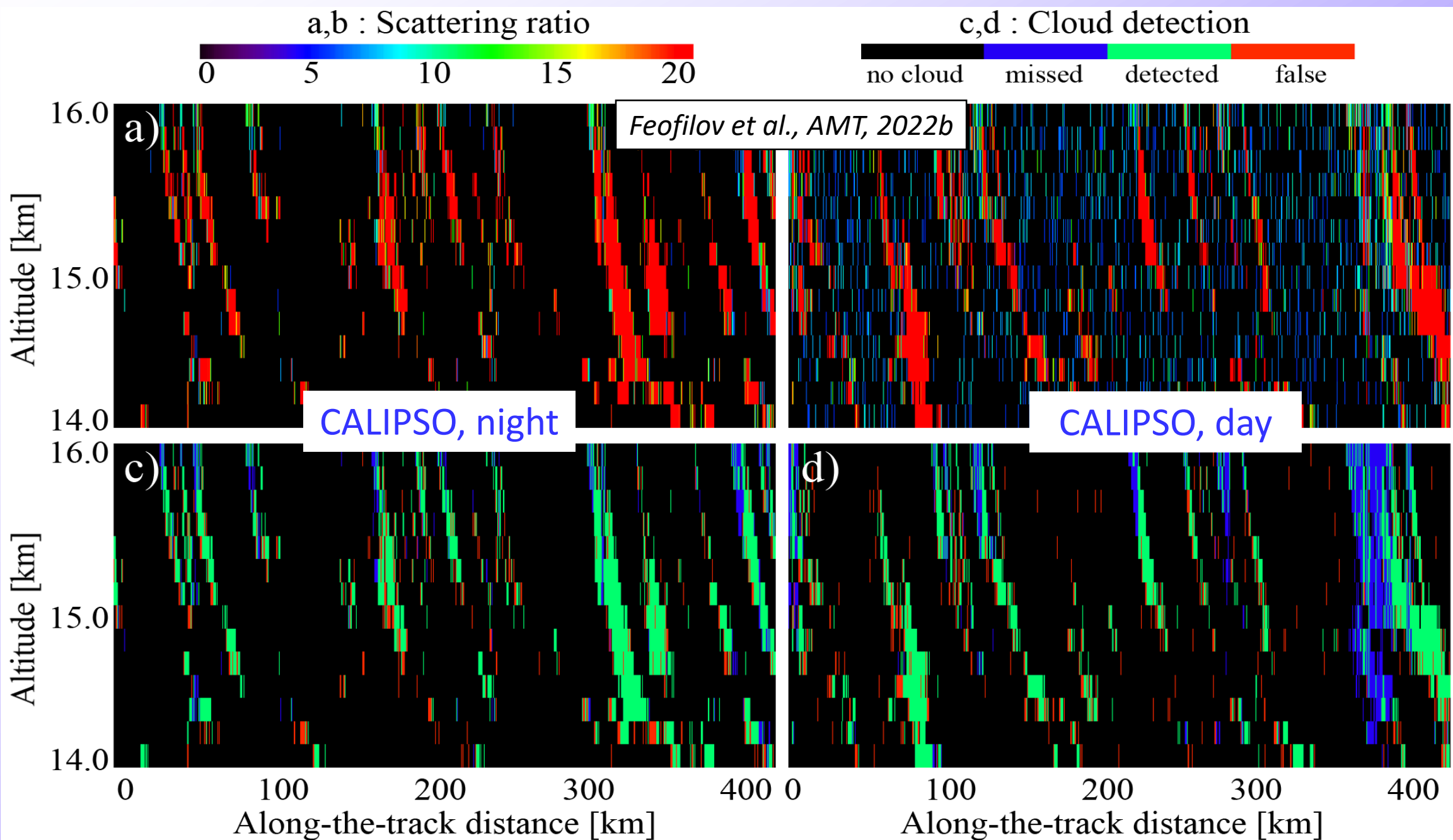
Modeling cloud observation at high resolution

Feofilov et al., AMT, 2022b

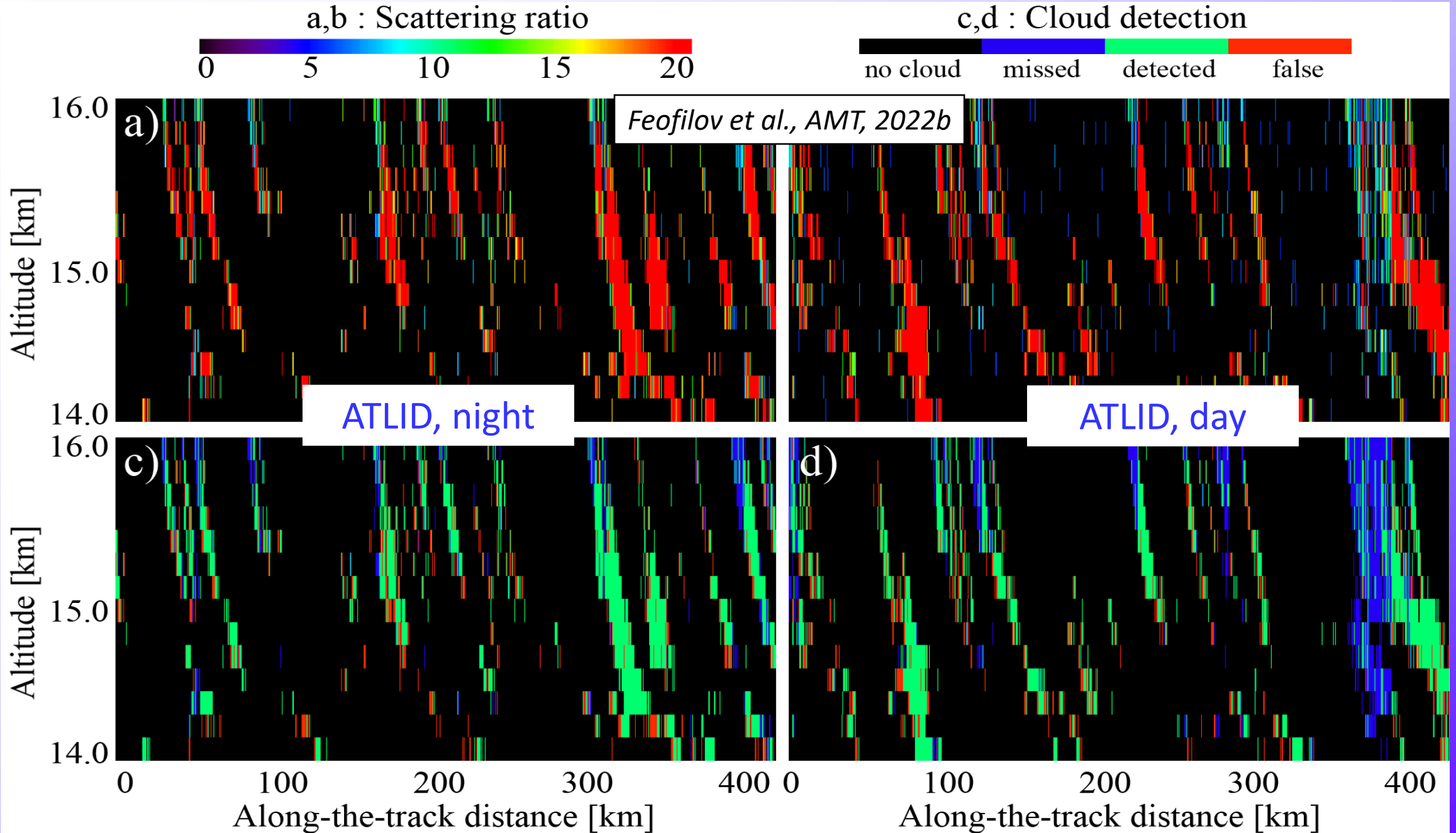


The 3DCLOUD_V3 model based on (Szczap et al., 2014; Alkasem et al., 2017) generates three-dimensional (3-D) spatial structures of stratocumulus and cirrus that share some statistical properties observed in real clouds.

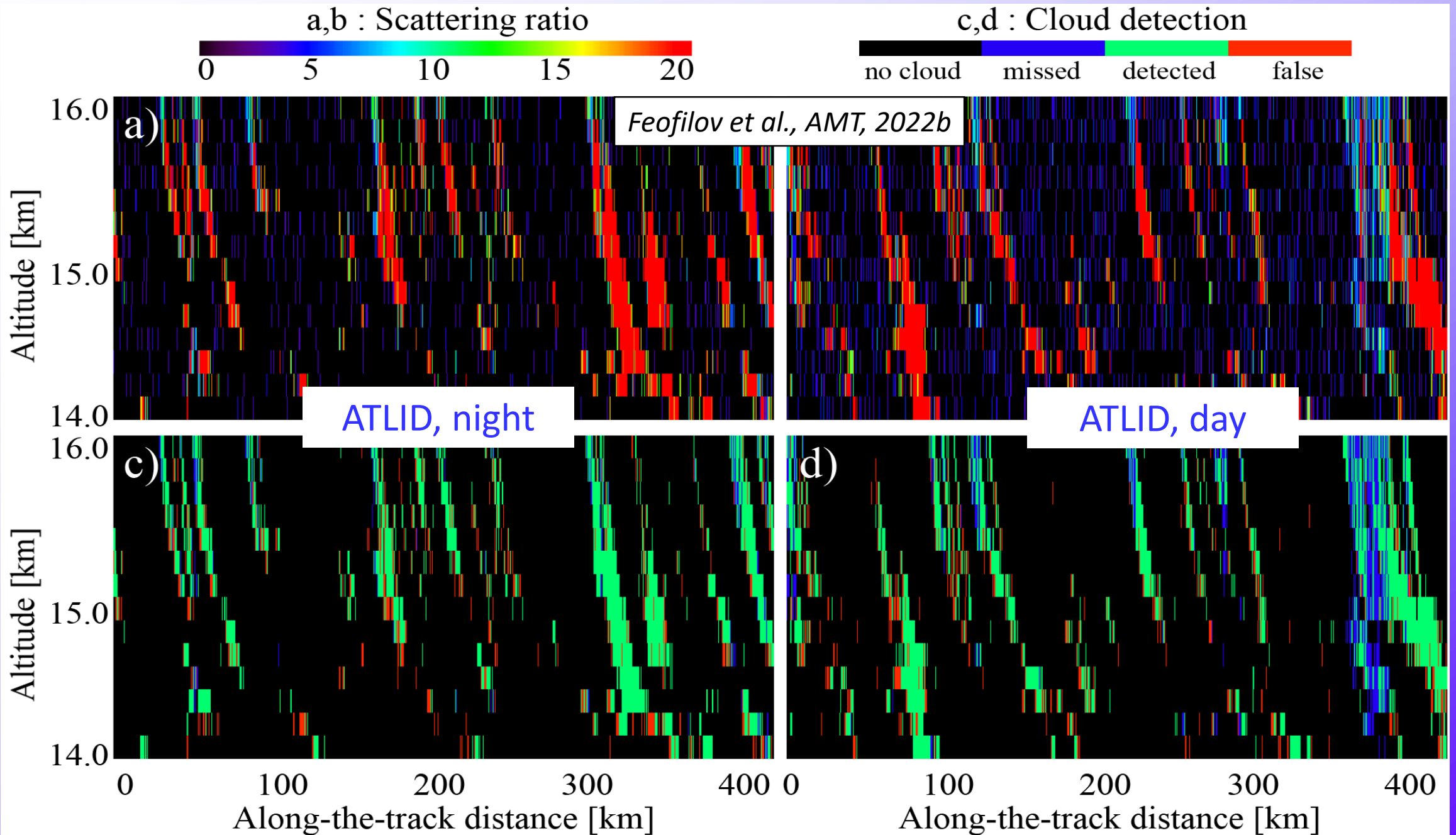
What to expect from ATLID w.r.t. CALIPSO, same SR threshold = 5



What to expect from ATLID w.r.t. CALIPSO, same SR threshold =5



If needed, SR threshold for ATLID can be lowered to 3



Take home messages

- To detect long-term trends in cloud radiative effects and feedbacks, one needs to merge cloud records from several lidars.
- The merging procedure should take into account the instrumental difference, the diurnal cycle, and averaging effects.
- Compensating for depolarization effects **significantly** improves the agreement in high clouds between ALADIN and CALIOP
- Compensating for diurnal cycle effects using AIRS/IASI improves the agreement between CALIOP and ALADIN over land where the difference in cloud amount is up to 20%.
- According to theoretical estimates, the daytime SNR of ATLID should be higher than that of CALIOP. Besides ensuring the continuity of cloud observations, this allows lowering SR threshold to detect thinner clouds.